Am J Cardiovasc Dis 2021;11(3):283-294
www.AJCD.us /ISSN:2160-200X/AJCD0133396

Original Article

Prevalence and prognostic impact of apical sparing contractility pattern in patients with aortic stenosis referred for transcatheter aortic valve implantation

Vera V Ferreira, Sílvia A Rosa, Tiago Pereira-da-Silva, Inês Rodrigues, António V Gonçalves, Tiago Mendonça, Alexandra Castelo, Luísa M Branco, Ana Galrinho, António Fiarresga, Ruben Ramos, Lino Patrício, Duarte Cacela, Rui C Ferreira

Department of Cardiology, Hospital de Santa Marta, Centro Hospitalar Universitário de Lisboa Central, Lisbon, Portugal

Received March 22, 2021; Accepted May 5, 2021; Epub June 15, 2021; Published June 30, 2021

Abstract: Introduction: Prolonged afterload increase in aortic stenosis (AS) may alter left ventricular (LV) contractility, irrespective of LV ejection fraction (LVEF). The prevalence and morbimortality associated with the apical sparing strain pattern (ASP), a typical finding of cardiac amyloidosis (CA), are not fully understood in patients with AS. We assessed the prevalence of the ASP in patients with severe AS and its clinical impact after transcatheter aortic valve implantation (TAVI). Methods: Eighty-nine consecutive patients with severe AS and LV hypertrophy referred for TAVI were included. Baseline clinical and echocardiographic data were assessed, including the ASP in bull's eye plots (ASPB), relative apical longitudinal strain (RALS) and EF to global longitudinal strain (EF/GLS) ratio. We analysed all-cause mortality; a composite of all-cause mortality, stroke, and heart failure hospitalizations; and the rate of pacemaker implantation, after TAVI. Results: Mean age was 82 ± 6 years and mean LVEF was 57 ± 10%. ASPB and RALS >1 were present in 43.8% and 24.7% of patients, respectively. Over a median follow-up of 13 months (IQR 6-32), ASPB was associated with higher rates of all-cause mortality (log-rank P=0.001) and was an independent predictor of all-cause mortality in multivariate analysis. Combination of the ASPB and GLS or EF/GLS ratio improved the risk stratification. Patients with RALS >1 were more likely to have new BBB and an indication for pacemaker implantation (P=0.048). Conclusion: The ASP, as assessed by the ASPB and RALS, was frequent in patients with AS regardless of the diagnosis of CA. The ASPB may refine risk stratification in patients referred for TAVI.

Keywords: Apical sparing, aortic stenosis, cardiac amyloidosis, strain echocardiography, transcatheter aortic valve implantation

Introduction

Aortic stenosis (AS) is the most common valvular disease in the developed countries [1, 2]. Longstanding AS promotes a sequence of adaptative reactions to pressure overload, inducing abnormal left ventricular (LV) compliance, diastolic dysfunction and impaired contractility [3]. Speckle tracking analysis allows for an evaluation of myocardial deformation, being a sensitive marker of regional and global LV systolic function [4, 5].

Prior studies have proposed that global myocardial deformation parameters and regional strain ratios, including relative apical sparing pattern (ASP), may have a better capacity in detecting and differentiating cardiac amyloidosis (CA) from other causes of LV hypertrophy [6-9]. LV longitudinal and circumferential strain is diminished in patients with CA, with the most pronounced impairment occurring in the basal segments and preservation of the cardiac apex contractility [10]. A relative ASP of LV longitudinal strain (LS) has shown accuracy and reproducibility for differentiating CA from other chronic pressure overload substrates. Based on this concept, Phelan D and coworkers [9] introduced the concept of relative apical longitudinal strain (RALS), and a RALS >1.0 was sensitive and specific in distinguishing CA from other entities presenting with increased LV wall

thickness (LVWT). Increased RALS was associated with worse outcomes in CA [11]. In addition, Pagourelias ED et al. [12] have proposed the ejection fraction to global longitudinal strain (EF/GLS) ratio for differentiating thickened hearts, and the cut off value of EF/GLS >4.1 showed good discriminating capacity in a mixed group of patients with CA and hypertrophic cardiomyopathy.

Despite the accuracy of the aforementioned parameters for detecting CA, including the ASBP, RALS and EF/GLS, some patients with AS may present with regional impairment patterns that closely resemble CA [6]. In fact, Lafitte S et al. [13] demonstrated that patients with severe AS and preserved left ventricular ejection fraction (LVEF) had lower global longitudinal strain (GLS) compared with controls and this difference was more pronounced in the basal LV segments. There are very few data about the prevalence and prognosis impact of typical CA echocardiographic myocardial deformation patterns in AS patients.

We aimed to evaluate the prevalence and prognostic impact of ASP in patients with severe AS undergoing transcatheter aortic valve implantation (TAVI).

Material and methods

Study design

This study was conducted at Centro Hospitalar Universitário de Lisboa Central, according to the institutional research policy (INV. Política de Investigação) and guideline for research of investigator initiative (INV. 101 Realização no CHULC de estudos clínicos da iniciativa do investigador). The project conformed to the principles outlined in the Helsinki Declaration. All the participants signed informed consent forms.

We retrospectively assessed patients with symptomatic severe AS referred for TAVI between 2012 and 2017 at a single tertiary care center. We selected patients with severe AS (defined according to European guideline on valvular heart disease [14]) and a maximum LVWT >12 mm. Exclusion criteria were as follows: severe LV dysfunction (LVEF <30%); history of myocardial infarction or wall motion abnormalities compatible with ischemic heart disease; and myocardial diseases, including a previous diagnosis of CA.

For each patient, clinical data including demographic characteristics and comorbidities were collected. Laboratory results and echocardiographic data preceding valvular treatment were also recorded.

For the assessment of the ASP, the presence of apical sparing pattern in bull's eye plots (ASPB), RALS, and EF/GLS ratio were evaluated.

Transthoracic echocardiogram (TTE)

A comprehensive TTE was performed before valvular treatment using commercially available ultrasound systems (Vivid 9 or Vivid E95; General Electric). Standard measurements of cardiac dimensions and function and classification of LV geometry were performed according to the recommendations of the European Association of Cardiovascular Imaging [15]. The LVEF was determined using Simpson's biplane method. Transaortic gradients were obtained using continuous wave Doppler and the simplified Bernoulli equation, while aortic valve area (AVA) was determined using the continuity equation.

2D speckle-tracking strain analysis

Speckle strain imaging was performed in patients with adequate endomyocardial border definition in transthoracic echocardiography using three standard apical views (**Figure 1A-C**). A semi-automatic tracing of the LV endocardium following manual delineation of the mitral valve edges and apex was undertaken. A "bull's eye" plots illustrating segmental LS values was automatically generated. Regional LS was determined in 17 segments of the LV according to published guidelines [15]. GLS was calculated as the average of segmental peak strain. The LS values for the 6 basal, 6 mid- and 5 apical segments of the LV were averaged to obtain regional LS (basal, mid, and apical, respectively).

Conventionally, the peak LS spectrum consists of a red-to-blue scale (-20% to 20%), representing the percent strain, where red colour denotes systolic longitudinal shortening, a greater shortening is shown as a darker shade of red, and lengthening (dyskinesis) is displayed in

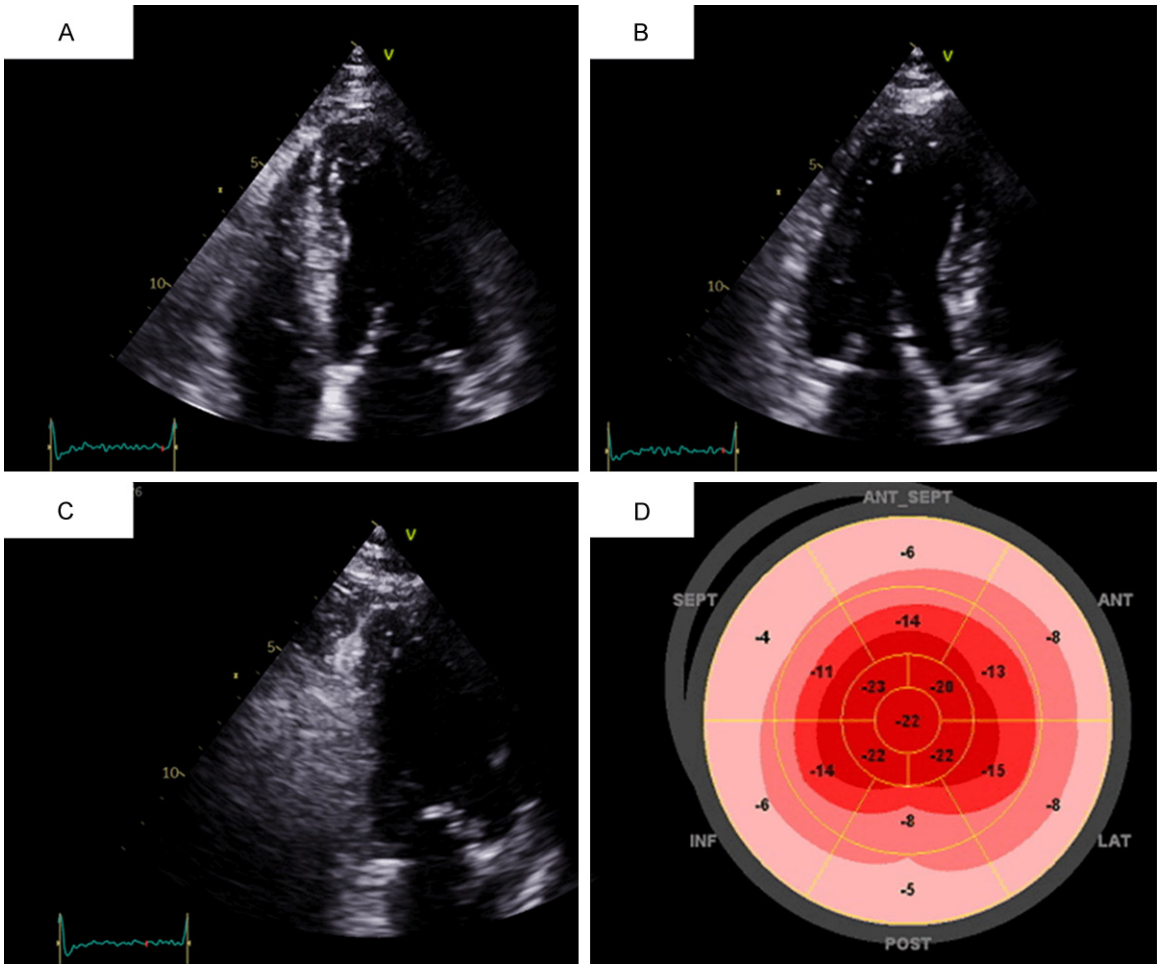

Figure 1. Apical sparing pattern of global LS in a patient with severe AS. Note the base-to-apex strain gradient, in which apical segments shows more normal strain compared with progressively worse values at the mid and basal segments. In this patient, average global LS was -13.0% and RALS was 1.16. The LV endocardium was manually identified in 4, 3 and 2-chamber (A-C, respectively) and tissue speckles were automatically tracked frame by frame throughout the cardiac cycle. A "bull's eye" plots illustrating segmental LS values was automatically generated (D). Global LS was calculated as the average LS of these 17 segments. RALS was calculated as [average apical LS/(average basal LS + average mid LS)]. LS: longitudinal strain, AS: aortic stenosis, LV: left ventricle, RALS: relative apical longitudinal strain.

shades of blue. The presence of ASPB was defined as a visually reduced LS in the basal and middle segments, as a pink or blue display, and a preserved LS in the apical segments, displayed in red [16] (**Figure 1D**). Two blinded sonographers assessed independently the presence of ASPB. RALS was calculated as [average apical LS/(average basal LS + average mid LS)] and a value of RALS >1.0 was defined as positive [9].

Clinical outcomes

Clinical endpoints were assessed by clinical appointments and by telephonic contact. The endpoints were all-cause mortality; a composite of all-cause mortality, stroke, and heart failure hospitalizations; and the rate of pacemaker implantation, after TAVI.

Statistical analysis

Continuous variables were expressed as the mean ± SD when normality was verified or as median (interquartile range (IQR)) when normality was not verified (Shapiro-Wilk or Kolmogorov-Smirnov tests). Categorical data are presented as frequency (percentage). For comparisons of continuous variables between groups, the student's T-test was used in nor-

Table 1. Clinical characteristics and baseline laboratory results of the studied cohort

	N=89
Clinical characteristics	
Age, years	82.1 ± 5.9
Male gender, n (%)	39 (43.8%)
Body mass index, kg/m^2	27.1 ± 4.5
Hypertension, n (%)	77 (86.5%)
Diabetes mellitus, n (%)	25 (28.1%)
Dyslipidemia, n (%)	57 (64.0%)
Smoking history, n (%)	15 (16.9%)
Coronary artery disease, n (%)	46 (51.7%)
Previous coronary artery bypass grafting, n (%)	15 (16.9%)
Previous stroke, n (%)	9 (10.1%)
Atrial fibrillation, n (%)	23 (25.8%)
Previous pacemaker implantation, n (%)	10 (11.2%)
NYHA class III-IV, n (%)	64 (71.9%)
Short-Term Risk score, %	5.5 ± 3.4
Laboratory results	
Hemoglobin, g/dL	12.0 ± 1.8
Creatinine, mg/dL	1.2 ± 0.8
Estimated glomerular filtration rate, ml/min	52.4 ± 21.9
Brain natriuretic peptide, ng/mL	646.4 ± 681.8

NYHA: New York Heart Association.

Table 2. Echocardiographic parameters of the studied cohort

Echocardiographic parameters	N=89
Aortic valve area, cm^2	0.6 ± 0.2
Maximum AG, mmHg	91.7 ± 24.4
Mean AG, mmHg	57.0 ± 16.8
Maximum LVWT, mm	14.6 ± 1.9
LVEDD, mm	51.9 ± 6.8
LVESD, mm	31.7 ± 6.8
LVEF, %	56.7 ± 10.0
LV mass, g	288.0 ± 72.1
Left atrial size, mm	45.8 ± 7.7
Aorta dimension, mm	30.9 ± 4.0
Pulmonary artery systolic pressure, mmHg	45.1 ± 14.1
Mean GLS, %	-13.0 ± 3.8
RALS, n (%)	0.78 ± 0.25
RALS >1, n (%)	22 (24.7%)
ASPB, n (%)	39 (43.8%)
EF/GLS, n (%)	4.7 ± 1.5
EF/GLS >4.1, n (%)	50 (56.2%)

AG: aortic gradient, LVWT: left ventricular wall thickness, LVESD: left ventricular end-systolic dimension, LVEF: left ventricular ejection fraction, GLS: global longitudinal strain, LS: longitudinal strain, RALS: relative apical longitudinal strain, ASPB: apical sparing pattern in bull's eye plots.

mally distributed variables and the Mann-Whitney test was used in variables without a normal distribution. Pairing of baseline characteristics and outcomes was performed using a chi-square test or Fisher's exact test for categorical variables. Survival after TAVI was estimated using a Kaplan-Meier curve and the curves were compared using a log-rank test. Univariable and multivariable Cox regression analyses were performed to identify predictors of all-cause mortality. A *p*-value of less than 0.05 was considered statistically significant. All statistical analyses were performed using dedicated software (SPSS Statistics, v. 25; IBM SPSS).

Results

Clinical and echocardiographic data

Of a sample of 108 patients, 19 patients were excluded due to severe LV dysfunction (2), previously diagnosed myocardiopathy (2), previous myocardial infarction (7), and inadequate endomyocardial border definition for LS measurements by TTE (8). A total of 89 patients were included, including 39 (43.8%) males, with a mean age of 82 ± 6 years.

The prevalence of coronary artery disease was 51.7% and 16.9% had undergone previous coronary artery bypass grafting. Regarding the functional capacity, 71.9% were in New York Heart Association (NYHA) functional class III or IV. Mean Short-Term Risk score was 5.5 ± 3.4%. Baseline clinical and laboratory data are summarized in **Table 1**.

Echocardiographic data

Table 2 presents the results of TTE analysis. The mean LVWT was 14.6 ± 1.9 mm. Mean LVEF was 56.7 ± 10.0% and 21 (23.6%) patients presented with LVEF <50%. The average maximum and mean transvalvu-

lar gradients were 91.7 ± 24.4 mmHg and 57.0 ± 16.8 mmHg, respectively, and the mean AVA was 0.6 ± 0.2 cm^2. Paradoxical low-flow, low-gradient aortic stenosis (PLFLG-AS) was found in 7 (7.9%) patients.

The average GLS was -13.0 ± 3.8% and 69.7% of patients had a GLS >-14.8%. The ASPB was present in 39 (43.8%) patients. The mean RALS was 0.78 ± 0.25. A RALS >1 was identified in 22 (24.7%) patients. An EF/GLS ratio >4.1 was observed in 50 (56.2%) patients.

Subgroups analysis

Age, gender, and the prevalence of cardiovascular risk factors did not differ according to presence of ASP in bull's eye plots (**Table 3**). Patients with ASPB showed a trend for increased prevalence of atrial fibrillation and significantly lower haemoglobin values at baseline. No significant differences in other comorbidities or laboratory data were registered. Patients with ASPB presented smaller LV systolic and diastolic diameters and showed a trend for increased LVWT. The LV mass, parameters reflecting the severity of valvular disease, LV systolic function, and post-procedural leak were not statistically different between the two groups. The prevalence of ASPB was similar in patients with and without PLFLG-AS (43.9% and 43.8%, P=0.957).

In the strain analysis, mean GLS tended to be more impaired in the ASPB group (-12.1 ± 3.0% vs -13.6 ± 4.2%, P=0.065) with 82.1% of patients having a mean GLS >-14.8% in such group.

Comparing patients according RALS >1 or ≤1, no significant differences were observed regarding the prevalence of hypertension, atrial fibrillation, chronic kidney disease and previous stroke. Echocardiographic parameters reflecting the severity of valvular disease, presence of PLFLG-AS, and rate of post-procedural leak did not differ between groups. Similarly to the ASPB subgroup, the maximum LVWT tended to be superior in RALS >1 group, while LV cavities tended to be smaller.

Outcomes

During a median follow-up of 13.4 months (IQR 6.4-32.2 months), 16 (18.0%) all-cause deaths, 21 (23.6%) events of composite endpoint, and 40 cases of new bundle branch block or pacemaker implantation occurred.

Kaplan-Meier survival analysis showed that the presence of ASPB was associated with increased all-cause mortality (log-rank P= 0.001, **Figure 2A**), including cardiovascular mortality (log-rank P=0.001, **Figure 2C**) and a trend for higher rates of the composite endpoint (log-rank P=0.067, **Figure 2B**).

The presence of RALS >1 was not associated with significantly increased rates of all-cause mortality, cardiovascular mortality, or the composite endpoint (**Figure 2D-F**). Of note, the incidence of new BBB and indication for pacemaker implantation at 12 months was higher in this subgroup (66.7% vs 41.3%, P=0.048).

The combination of GLS and ASPB further refined the risk stratification. Patients with GLS >-14.8% and ASPB had significantly worse prognosis regarding all-cause mortality compared with other patients (log-rank P=0.010, **Figure 3A**). In addition, the presence of ASPB and EF/GLS ratio >4.1 was associated with the worst prognosis, while the absence of both was linked to a better outcome (log-rank P=0.011, **Figure 3B**).

In multivariate Cox regression analysis, ASPB was associated with all-cause mortality (HR 5.04, 95% CI 1.40-18.21, P=0.014), along with diabetes mellitus (HR 0.10, 95% CI 0.01-0.80, P=0.030), and atrial fibrillation (HR 2.90, 95% CI 1.03-8.22, P=0.045, **Tables 4** and **5**).

Discussion

Our study has three main findings. First, in our cohort of patients with severe AS referred for TAVI, imaging parameters of ASP were frequent, and their prevalence did not differ according to the presence of PLFLG-AS. Second, the presence of ASP in patients with AS was associated with significantly increased all-cause mortality after valvular treatment. Third, multiparametric imaging combining GLS or EF/GLS and ASP improved risk stratification.

From a pathophysiology perspective, the pressure afterload generated by AS elicit a continuum of alterations from myocyte hypertrophy to a self-perpetuating process of myocyte atrophy,

Table 3. Comparison of subgroups of patients according to the presence of ASBP and RALS >1

	ASPB N=39	No ASPB N=50	*p-value*	RALS >1 N=22	RALS ≤1 N=67	*p-value*
Clinical characteristics						
Age, years	81.6 ± 6.1	82.4 ± 5.8	0.537	80.8 ± 7.4	82.5 ± 5.3	0.254
Male gender, n (%)	22 (56.4%)	28 (56.0%)	0.969	10 (45.5%)	29 (43.3%)	0.859
Body mass index, kg/m^2	27.0 ± 4.5	27.1 ± 4.5	0.910	26.2 ± 4.6	27.4 ± 4.4	0.266
Hypertension, n (%)	32 (82.1%)	45 (90.0%)	0.282	18 (81.8%)	59 (88.1%)	0.460
Diabetes mellitus, n (%)	10 (25.6%)	15 (30.0%)	0.650	3 (13.6%)	22 (32.8%)	0.093
Dyslipidemia, n (%)	22 (56.4%)	35 (70.0%)	0.187	11 (50%)	46 (68.7%)	0.118
Smoking history, n (%)	7 (17.9%)	8 (16.0%)	0.808	3 (13.6%)	12 (17.9%)	0.643
Coronary disease, n (%)	20 (51.3%)	26 (52.0%)	0.946	9 (40.9%)	37 (55.2%)	0.247
Previous coronary artery bypass grafting, n (%)	6 (15.4%)	9 (18.0%)	0.744	2 (9.1%)	13 (19.4%)	0.274
Previous stroke, n (%)	3 (7.7%)	6 (12.0%)	0.507	2 (9.1%)	7 (10.4%)	0.855
Atrial fibrillation, n (%)	14 (35.9%)	10 (20.0%)	0.059	7 (31.8%)	16 (23.9%)	0.462
Previous pacemaker implantation, n (%)	2 (5.1%)	8 (16.0%)	0.125	1 (4.5%)	9 (13.4%)	0.276
NYHA class III-IV. n (%)	31 (79.5%)	33 (66.0%)	0.164	16 (72.7%)	48 (71.6%)	0.922
Short-Term Risk score, %	5.2 ± 3.0	5.8 ± 3.7	0.381	5.0 ± 3.3	5.7 ± 3.4	0.414
Laboratory results						
Hemoglobin, g/dL	11.5 ± 1.9	12.4 ± 1.7	0.025	11.7 ± 1.9	12.1 ± 1.8	0.416
Creatinine, mg/dL	1.11 ± 0.35	1.26 ± 1.04	0.429	1.0 ± 0.3	1.3 ± 0.9	0.178
Estimated glomerular filtration rate, ml/min	51.4 ± 20.2	53.3 ± 23.4	0.696	56.0 ± 25.2	51.2 ± 20.8	0.370
Brain natriuretic peptide, ng/mL	759.1 ± 670.4	561.9 ± 685.1	0.199	719.3 ± 645.7	623.6 ± 696.1	0.583
Echocardiographic parameters						
Aortic valve area, cm^2	0.6 ± 0.2	0.7 ± 0.2	0.774	0.7 ± 0.3	0.6 ± 0.2	0.556
Maximum AG, mmHg	92.1 ± 26.2	91.4 ± 23.2	0.894	90.3 ± 23.9	92.1 ± 24.8	0.774
Mean AG, mmHg	58.3 ± 18.1	56.1 ± 15.8	0.551	56.8 ± 17.4	57.1 ± 16.8	0.939
Maximum LVWT, mm	15.0 ± 2.2	14.3 ± 1.5	0.068	15.2 ± 2.6	14.4 ± 1.5	0.091
Paradoxical low-flow, low-gradient aortic stenosis, n (%)	3 (42.9%)	4 (57.1%)	0.957	2 (28.6%)	5 (71.4%)	0.806
LVESD, mm	29.7 ± 6.0	33.2 ± 7.0	0.020	29.3 ± 5.2	32.4 ± 7.1	0.067
LVEDD, mm	50.1 ± 6.3	53.3 ± 6.9	0.029	51.1 ± 5.2	52.1 ± 7.3	0.550
LVEF, %	56.8 ± 9.9	56.7 ± 10.1	0.940	58.6 ± 9.6	56.1 ± 10.1	0.313
LV mass, g	278.3 ± 75.1	296.3 ± 69.5	0.357	304.0 ± 64.7	282.4 ± 74.4	0.333
Left atrial size, mm	46.8 ± 8.8	44.9 ± 6.7	0.347	46.3 ± 8.7	45.6 ± 7.5	0.740
Aorta dimension, mm	30.3 ± 4.2	31.4 ± 3.8	0.274	31.2 ± 4.2	30.8 ± 4.0	0.680
Pulmonary artery systolic pressure, mmHg	46.3 ± 13.7	44.0 ± 14.5	0.487	44.3 ± 12.2	45.5 ± 14.8	0.756
Mean GLS, %	-12.1 ± 3.0	-13.6 ± 4.2	0.065	-13.5 ± 3.1	-12.8 ± 4.0	0.419
Mean GLS >-14.8%, n (%)	32 (82.1%)	30 (60.0%)	0.028	15 (68.2%)	47 (70.1%)	0.862
Mean basal LS, %	-7.5 ± 1.9	-11.3 ± 3.0	0.001	-7.4 ± 2.3	-10.3 ± 3.1	0.001
Mean mid LS, %	-11.7 ± 2.7	-13.6 ± 4.2	0.020	-12.5 ± 2.8	-12.8 ± 4.0	0.769
Mean apical LS, %	-18.2 ± 5.6	-16.5 ± 7.0	0.213	-22.1 ± 5.0	-15.7 ± 6.1	0.001
RALS, n (%)	0.95 ± 0.21	0.64 ± 0.19	0.001	1.12 ± 0.13	0.67 ± 0.16	0.001
EF/GLS	5.0 ± 1.6	4.5 ± 1.4	0.117	4.7 ± 1.8	4.7 ± 1.4	0.885
EF/GLS >4.1, n (%)	26 (66.7%)	24 (48.0%)	0.080	11 (50%)	39 (58.2%)	0.502
Post-procedural leak, n (%)						
Any	10 (25.7%)	16 (32.0%)	0.242	6 (27.3%)	20 (29.9%)	0.650
Moderate or severe	1 (2.6%)	6 (12.0%)	0.136	1 (4.5%)	6 (9.0%)	0.513

NYHA: New York Heart Association, AG: aortic gradient, LVWT: left ventricular wall thickness, LVESD: left ventricular end-systolic dimension, LVEF: left ventricular ejection fraction, GLS: global longitudinal strain, LS: longitudinal strain, RALS: relative apical longitudinal strain, ASPB: apical sparing pattern in bull's eye plots, BBB: bundle branch block.

cell death and resultant replacement fibrosis [17]. Current data advocates that GLS is compromised due to increased afterload, mainly in the basal segments of the LV septum where wall stress is maximal [8]. It is still incompletely understood if there is a causal relationship between AS and CA and whether CA is a cause or a consequence of AS. Indeed, both are frequently observed in the elderly and there is increasing evidence in the literature establish-

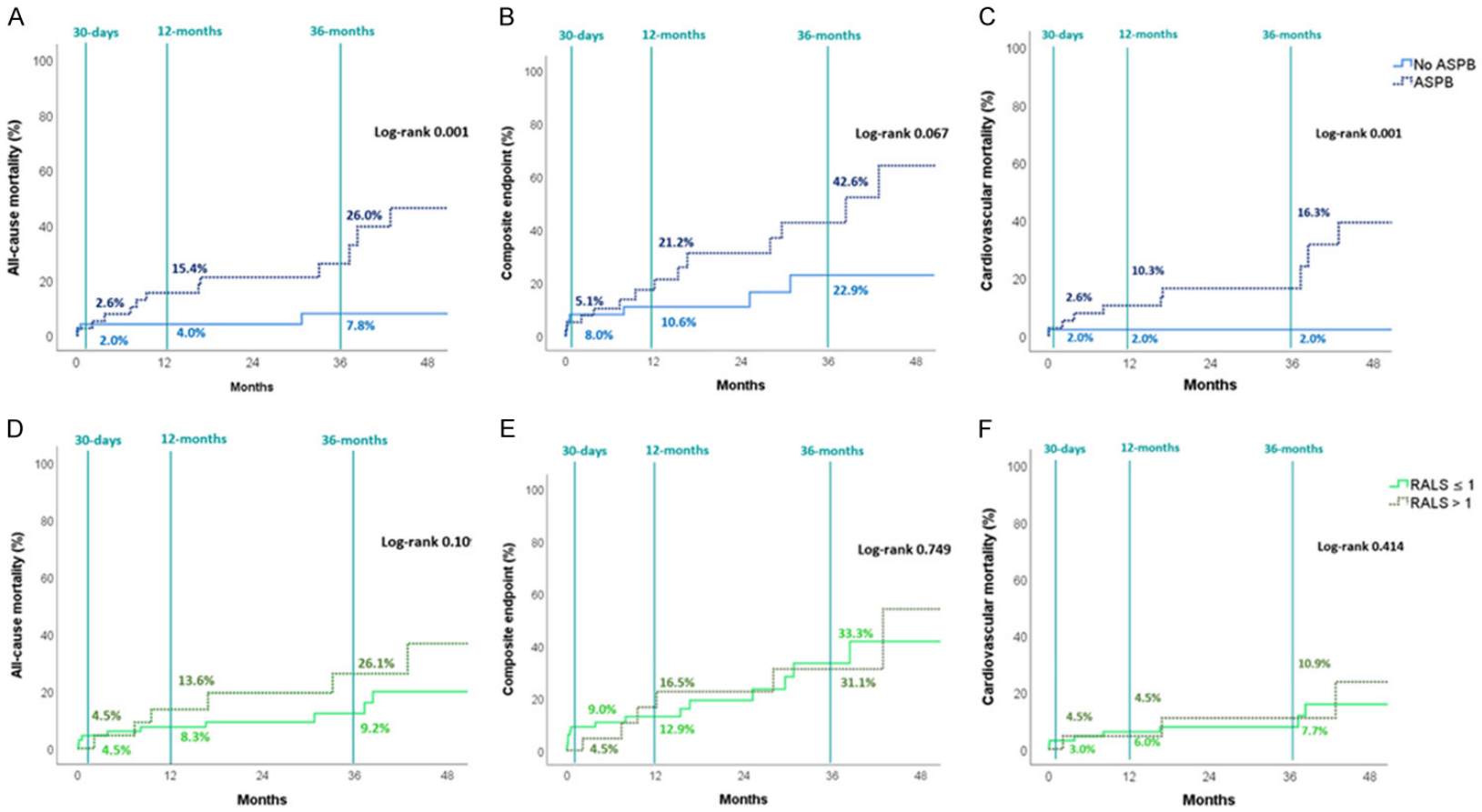

Figure 2. Kaplan-Meier curves for outcomes concerning the presence of ASPB and RALS >1. Upper row shows Kaplan-Meier analyses for patients stratified according to the presence of APSB, regarding the incidence of all-cause mortality (A), composite endpoint (B) and cardiovascular mortality (C). Bottom row represent Kaplan-Meier curves stratified according to the presence of RALS >1, regarding all-cause mortality (D), composite endpoint (E) and cardiovascular mortality (F). ASPB: apical sparing pattern in bull's eye plots, RALS: relative apical longitudinal strain.

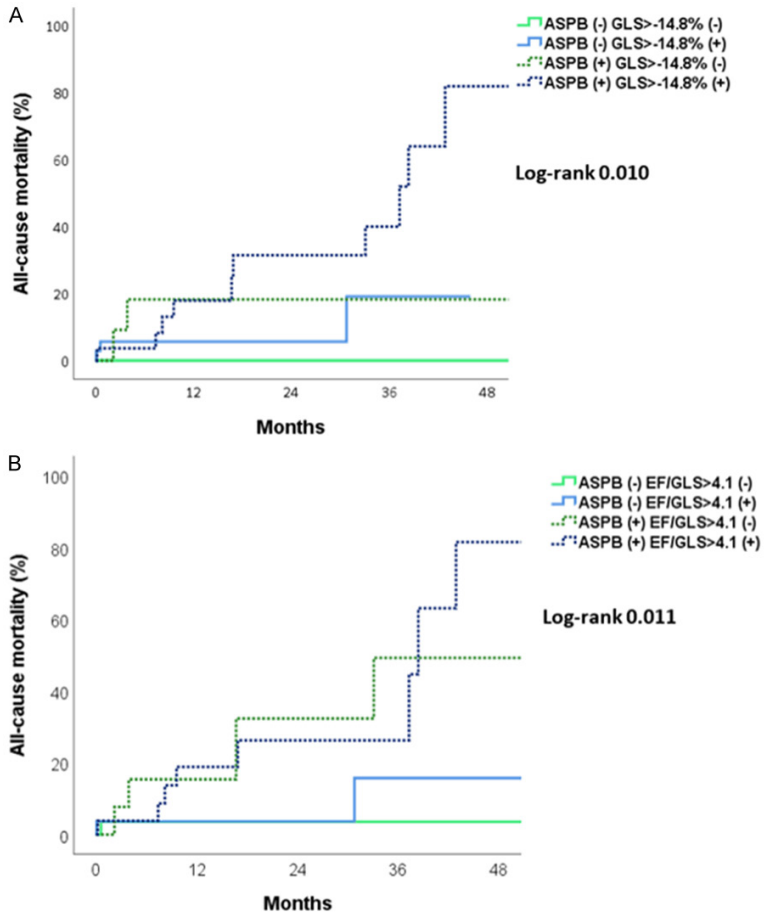

Figure 3. Kaplan-Meier analyses for patients stratified according to the presence of (A) APSB and GLS >-14.8%, or (B) APSB and EF/GLS ratio >4.1. ASPB: apical sparing pattern in bull's eye plots, GLS: global longitudinal strain, EF/GLS: ejection fraction/global.

ing a crucial role of oxidative stress, inflammation and extracellular matrix turnover in both the transthyretin (TTR) amyloidogenic process [18] and pathophysiology of AS [19, 20]. It is also likely that amyloid deposits could be induced or accelerated in AS. This is supported by the recognition of a high prevalence of TTR amyloid deposits in samples of septal myectomy and in heart valves during surgical aortic valve replacement for AS [21, 22]. On one hand, the amyloid deposits could induce or worsen AS and, on the other hand, shear stresses induced by AS could have detrimental effects on myocardial remodelling and could lead to TTR amyloid deposits [22, 23]. In this subgroup of AS patients, ASP may traduce ventricular wall stress related to increased pressure overload, fibrosis or amyloid infiltration, and conducts to maladaptive responses such as inappropriate LV hypertrophy and impaired contractility.

In our study, ASP in bull's eye plots was registered in 43.8% of patients. In contrast with some previous data, we did not find any association between these parameters and age, gender, or the presence of PLFLG-AS [24-26]. The prevalence of CA reported in prior studies reached 25% in octogenarian, being probably underestimated due to the absence of systematic screening, the complexity of diagnosis workup and the overlap with other hypertrophic substrates [27-29]. In our study, no significant differences with respect to other conventional risk factors and comorbidities were registered, except for lower hemoglobin values in patients with ASPB.

The relationship between the presence of ASP and worse long-term outcomes has been formerly described in CA patients [30-34]. In line with published data, our patients with ASPB also presented worse prognosis. Besides the presence of diabetes and atrial fibrillation, no other clinical laboratory or imaging data were associated with all-cause mortality, as registered in prior studies [24, 28]. This could be due to the reduced dimension of our sample. Notably, ASPB was an independent predictor of all-cause mortality after adjusting for other clinical, laboratory, and imaging parameters. This highlights the importance of detecting subclinical LV disfunction, in particular the ASP, in this subgroup of patients.

A RALS >1 was present in about one-quarter of patients in this study. We noticed that patients who presented a RALS >1 tended to experience higher mortality (log-rank P=0.109), although this difference was not significant. Liu D et al. [11] also reported that higher RALS were associated with worse outcomes in patients with CA. We found that patients with RALS >1 were more likely to have new bundle branch block and an indication for pacemaker

Table 4. Identification of prognostic factors for all-cause mortality based on univariate Cox analysis

	Univariate Analysis	
	HR (95% CI)	*p-value*
Age, years	1.01 (0.93-1.10)	0.863
Male gender	0.87 (0.33-2.32)	0.777
Body mass index, kg/m^2	0.99 (0.88-1.12)	0.893
Hypertension	0.39 (0.13-1.23)	0.394
Diabetes mellitus	0.13 (0.02-1.00)	0.050
Dyslipidemia	2.00 (0.64-6.23)	0.232
Smoking history	1.69 (0.54-5.25)	0.367
Coronary disease	1.42 (0.514-3.91)	0.500
Previous coronary artery bypass grafting	0.89 (0.26-3.23)	0.894
Previous stroke	1.89 (0.42-8.49)	0.405
Atrial fibrillation	2.76 (1.02-7.44)	0.045
Previous pacemaker implantation	0.04 (0.00-42.21)	0.368
NYHA class III-IV	3.16 (0.72-13.95)	0.129
Short-Term Risk score	0.95 (0.81-1.11)	0.488
Hemoglobin, g/dL	0.72 (0.54-0.95)	0.020
Creatinine, mg/dL	1.11 (0.61-2.04)	0.726
Estimated glomerular filtration rate, ml/min	0.99 (0.97-1.02)	0.707
Brain natriuretic peptide, ng/mL	1.00 (1.00-1.00)	0.673
Aortic valve area, cm^2	5.84 (0.62-55.28)	0.124
Maximum AG, mmHg	0.99 (0.97-1.02)	0.535
Mean AG, mmHg	0.99 (0.97-1.03)	0.880
Maximum LVWT, mm	1.14 (0.92-1.40)	0.238
LVESD, mm,	0.98 (0.91-1.06)	0.596
LVEDD, mm	0.98 (0.92-1.06)	0.643
LVEF, %	1.01 (0.95-1.05)	0.994
LV mass, g	1.00 (0.99-1.01)	0.730
Left atrial size, mm	1.01 (0.93-1.08)	0.905
Aorta dimension, mm	1.04 (0.90-1.19)	0.628
Pulmonary artery systolic pressure, mmHg	1.04 (1.00-1.07)	0.067
Mean GLS, %	1.00 (0.88-1.14)	0.964
Mean GLS >-14.8 %	2.08 (0.59-7.31)	0.255
Mean basal LS, %	1.18 (1.00-1.40)	0.055
Mean mid LS, %	1.04 (0.91-1.20)	0.531
Mean apical LS, %	0.99 (0.92-1.08)	0.846
ASPB	6.21 (1.77-21.83)	0.004
RALS >1	2.20 (0.82-5.93)	0.118
EF/GLS	1.07 (0.80-1.45)	0.648
EF/GLS >4.1	1.29 (0.47-3.54)	0.624
Post-procedural leak (moderate or severe)	0.21 (0.00-35.79)	0.554

NYHA: New York Heart Association, AG: aortic gradient, LVWT: left ventricular wall thickness, LVESD: left ventricular end-systolic dimension, LVEF: left ventricular ejection fraction, GLS: global longitudinal strain, LS: longitudinal strain, RALS: relative apical longitudinal strain, ASPB: apical sparing pattern in bull's eye plots HR: hazard ratio; CI: confidence interval.

implantation. From the pathophysiological basis, conduction disturbances in CA are known to be due to the infiltration of the conduction system by the deposits of amyloid fibrils and loss of autonomic nervous control of cardiac function [26]. This can explain the greater susceptibility for conduction disturbances after TAVI in RALS group.

A GLS impairment can be identified before the decrease of LVEF in patients with CA [35]. LS of LV assessed by speckle-tracking echocardiography is an independent predictor of mortality in amyloidosis [35, 36]. A GLS value higher than -14.81% has been shown to be a predictor of all-cause mortality among patients with CA with preserved LVEF [37]. In our sample of patients with AS, the concurrent presence of ASPB and GLS >-14.8%, as well as the coexistence of ASPB and EF/GLS ratio >4.1, were associated with significantly higher all-cause mortality.

The relationship between ASP and AS have not been well studied. The results of our study add important information to published data regarding outcomes of ASP in AS patients undergoing TAVI. Of LV strain parameters, the presence of ASPB, was associated with worse outcomes, irrespective of associated CA, after multivariate adjustment. Combination of the ASP and GLS or EF/GLS ratio further refined the risk stratification. Speckle tracking echocardiography provides an accessible and reliable assessment of these parameters, consisting a valuable non-invasive tool to stratify prognosis of this subset of patients.

Study limitations

The present work has some limitations. This was a retrospective study and, therefore,

Table 5. Identification of prognostic factors for all-cause mortality based on multivariate Cox analysis

	Multivariate Analysis	
	HR (95% CI)	*p-value*
Diabetes mellitus	0.10 (0.01-0.80)	0.030
Atrial fibrillation	2.90 (1.03-8.22)	0.045
ASPB	5.04 (1.40-18.21)	0.014

ASPB: apical sparing pattern in bull's eye plots; HR: Hazard ratio; CI: confidence interval.

unmeasured confounding factors may have influenced the observed associations. In addition, this was a single-center study and the sample size was not large. As previously stated, we excluded patients with previously known CA, although we cannot definitely exclude that some patients had undiagnosed CA, since histological diagnosis, DPD scan, or light chain analysis were not routinely performed. However, our goal was not to evaluate the real presence of CA or whether there is amyloid deposition but to assess an echocardiographic pattern of apical sparing and, ultimately, if such a strain pattern was associated with prognosis. Further studies are warranted to detect the prevalence of CA in AS patients referred for TAVI and the accuracy of ASP for diagnosing CA in such patients.

Conclusion

The apical sparing pattern was prevalent among elderly individuals with severe AS. Speckle tracking parameters, including apical sparing, global longitudinal strain and ejection fraction/GLS ratio, showed to be useful tools to stratify the prognosis of patients with AS undergoing TAVI. These parameters may therefore contribute to tailor therapeutic interventions in such group of patients.

Acknowledgements

The authors thank the study patients and investigators for their contributions to data collection and analysis, assistance with statistical analysis and critical review of the article.

Disclosure of conflict of interest

None.

Address correspondence to: Dr. Vera V Ferreira, Department of Cardiology, Hospital de Santa Marta. Rua de Santa Marta, nº 50, 1169-024, Lisbon, Portugal. Tel: +351 915761971; ORCID: https://orcid.org/0000-0002-8957-9279; E-mail: verasvferreira25@gmail.com

References

[1] D'Arcy JL, Coffey S, Loudon MA, Kennedy A, Pearson-Stuttard J, Birks J, Frangou E, Farmer AJ, Mant D, Wilson J, Myerson SG and Prendergast BD. Large-scale community echocardiographic screening reveals a major burden of undiagnosed valvular heart disease in older people: the OxVALVE population cohort study. Eur Heart J 2016; 37: 3515-3522.

[2] Thaden JJ, Nkomo VT and Enriquez-Sarano M. The global burden of aortic stenosis. Prog Cardiovasc Dis 2014; 56: 565-571.

[3] Badiani S, van Zalen J, Treibel TA, Bhattacharyya S, Moon JC and Lloyd G. Aortic stenosis, a left ventricular disease: insights from advanced imaging. Curr Cardiol Rep 2016; 18: 80.

[4] Kusunose K, Goodman A, Parikh R, Barr T, Agarwal S, Popovic ZB, Grimm RA, Griffin BP and Desai MY. Incremental prognostic value of left ventricular global longitudinal strain in patients with aortic stenosis and preserved ejection fraction. Circ Cardiovasc Imaging 2014; 7: 938-945.

[5] Ng ACT, Prihadi EA, Antoni ML, Bertini M, Ewe SH, Ajmone Marsan N, Leung DY, Delgado V and Bax JJ. Left ventricular global longitudinal strain is predictive of all-cause mortality independent of aortic stenosis severity and ejection fraction. Eur Heart J Cardiovasc Imaging 2018; 19: 859-867.

[6] Pagourelias ED, Mirea O, Duchenne J, Van Cleemput J, Delforge M, Bogaert J, Kuznetsova T and Voigt JU. Echo parameters for differential diagnosis in cardiac amyloidosis: a head-to-head comparison of deformation and nondeformation parameters. Circ Cardiovasc Imaging 2017; 10: e005588.

[7] Cariou E, Bennani Smires Y, Victor G, Robin G, Ribes D, Pascal P, Petermann A, Fournier P, Faguer S, Roncalli J, Rousseau H, Chauveau D, Carrié D, Berry I, Galinier M and Lairez O; Toulouse Amyloidosis Research Network collaborators *. Diagnostic score for the detection of cardiac amyloidosis in patients with left ventricular hypertrophy and impact on prognosis. Amyloid 2017; 24: 101-109.

[8] D'Andrea A, Radmilovic J, Ballo P, Mele D, Agricola E, Cameli M, Rossi A, Esposito R, Novo G, Mondillo S, Montisci R, Gallina S, Bossone E and Galderisi M; Working Group on Echocardiography of the Italian Society of Cardiology. Left ventricular hypertrophy or storage disease? The incremental value of speckle track-

ing strain bull's-eye. Echocardiography 2017; 34: 746-759.
[9] Phelan D, Collier P, Thavendiranathan P, Popovic ZB, Hanna M, Plana JC, Marwick TH and Thomas JD. Relative apical sparing of longitudinal strain using two-dimensional speckle-tracking echocardiography is both sensitive and specific for the diagnosis of cardiac amyloidosis. Heart 2012; 98: 1442-1448.
[10] Urbano-Moral JA, Gangadharamurthy D, Comenzo RL, Pandian NG and Patel AR. Three-dimensional speckle tracking echocardiography in light chain cardiac amyloidosis: examination of left and right ventricular myocardial mechanics parameters. Rev Esp Cardiol (Engl Ed) 2015; 68: 657-664.
[11] Liu D, Hu K, Niemann M, Herrmann S, Cikes M, Stork S, Gaudron PD, Knop S, Ertl G, Bijnens B and Weidemann F. Effect of combined systolic and diastolic functional parameter assessment for differentiation of cardiac amyloidosis from other causes of concentric left ventricular hypertrophy. Circ Cardiovasc Imaging 2013; 6: 1066-1072.
[12] Pagourelias ED, Duchenne J, Mirea O, Vovas G, Van Cleemput J, Delforge M, Kuznetsova T, Bogaert J and Voigt JU. The relation of ejection fraction and global longitudinal strain in amyloidosis: implications for differential diagnosis. JACC Cardiovasc Imaging 2016; 9: 1358-1359.
[13] Lafitte S, Perlant M, Reant P, Serri K, Douard H, DeMaria A and Roudaut R. Impact of impaired myocardial deformations on exercise tolerance and prognosis in patients with asymptomatic aortic stenosis. Eur J Echocardiogr 2009; 10: 414-419.
[14] Baumgartner H, Falk V, Bax JJ, De Bonis M, Hamm C, Holm PJ, Iung B, Lancellotti P, Lansac E, Rodriguez Muñoz D, Rosenhek R, Sjögren J, Tornos Mas P, Vahanian A, Walther T, Wendler O, Windecker S and Zamorano JL; ESC Scientific Document Group. 2017 ESC/EACTS Guidelines for the management of valvular heart disease. Eur Heart J 2017; 38: 2739-2791.
[15] Lang RM, Badano LP, Mor-Avi V, Afilalo J, Armstrong A, Ernande L, Flachskampf FA, Foster E, Goldstein SA, Kuznetsova T, Lancellotti P, Muraru D, Picard MH, Rietzschel ER, Rudski L, Spencer KT, Tsang W and Voigt JU. Recommendations for cardiac chamber quantification by echocardiography in adults: an update from the American Society of Echocardiography and the European Association of Cardiovascular Imaging. J Am Soc Echocardiogr 2015; 28: 1-39, e14.
[16] Lee GY, Kim HK, Choi JO, Chang SA, Oh JK, Jeon ES and Sohn DW. Visual assessment of relative apical sparing pattern is more useful than quantitative assessment for diagnosing cardiac amyloidosis in borderline or mildly increased left ventricular wall thickness. Circ J 2015; 79: 1575-1584.
[17] Hein S, Arnon E, Kostin S, Schonburg M, Elsasser A, Polyakova V, Bauer EP, Klovekorn WP and Schaper J. Progression from compensated hypertrophy to failure in the pressure-overloaded human heart: structural deterioration and compensatory mechanisms. Circulation 2003; 107: 984-991.
[18] Zhao L, Buxbaum JN and Reixach N. Age-related oxidative modifications of transthyretin modulate its amyloidogenicity. Biochemistry 2013; 52: 1913-1926.
[19] Park JY, Ryu SK, Choi JW, Ho KM, Jun JH, Rha SW, Park SM, Kim HJ, Choi BG, Noh YK and Kim S. Association of inflammation, myocardial fibrosis and cardiac remodelling in patients with mild aortic stenosis as assessed by biomarkers and echocardiography. Clin Exp Pharmacol Physiol 2014; 41: 185-191.
[20] Henderson BC, Tyagi N, Ovechkin A, Kartha GK, Moshal KS and Tyagi SC. Oxidative remodeling in pressure overload induced chronic heart failure. Eur J Heart Fail 2007; 9: 450-457.
[21] Allen RD, Edwards WD, Tazelaar HD and Danielson GK. Surgical pathology of subaortic septal myectomy not associated with hypertrophic cardiomyopathy: a study of 98 cases (1996-2000). Cardiovasc Pathol 2003; 12: 207-215.
[22] Kristen AV, Schnabel PA, Winter B, Helmke BM, Longerich T, Hardt S, Koch A, Sack FU, Katus HA, Linke RP and Dengler TJ. High prevalence of amyloid in 150 surgically removed heart valves--a comparison of histological and clinical data reveals a correlation to atheroinflammatory conditions. Cardiovasc Pathol 2010; 19: 228-235.
[23] Galat A, Guellich A, Bodez D, Slama M, Dijos M, Zeitoun DM, Milleron O, Attias D, Dubois-Rande JL, Mohty D, Audureau E, Teiger E, Rosso J, Monin JL and Damy T. Aortic stenosis and transthyretin cardiac amyloidosis: the chicken or the egg? Eur Heart J 2016; 37: 3525-3531.
[24] Cavalcante JL, Rijal S, Abdelkarim I, Althouse AD, Sharbaugh MS, Fridman Y, Soman P, Forman DE, Schindler JT, Gleason TG, Lee JS and Schelbert EB. Cardiac amyloidosis is prevalent in older patients with aortic stenosis and carries worse prognosis. J Cardiovasc Magn Reson 2017; 19: 98.
[25] Castano A, Narotsky DL, Hamid N, Khalique OK, Morgenstern R, DeLuca A, Rubin J, Chiuzan C, Nazif T, Vahl T, George I, Kodali S, Leon MB, Hahn R, Bokhari S and Maurer MS. Unveiling transthyretin cardiac amyloidosis and its predictors among elderly patients with severe aortic stenosis undergoing transcatheter aor-

tic valve replacement. Eur Heart J 2017; 38: 2879-2887.
[26] Ruberg FL, Grogan M, Hanna M, Kelly JW and Maurer MS. Transthyretin amyloid cardiomyopathy: JACC state-of-the-art review. J Am Coll Cardiol 2019; 73: 2872-2891.
[27] Mohammed SF, Mirzoyev SA, Edwards WD, Dogan A, Grogan DR, Dunlay SM, Roger VL, Gertz MA, Dispenzieri A, Zeldenrust SR and Redfield MM. Left ventricular amyloid deposition in patients with heart failure and preserved ejection fraction. JACC Heart Fail 2014; 2: 113-122.
[28] Treibel TA, Fontana M, Gilbertson JA, Castelletti S, White SK, Scully PR, Roberts N, Hutt DF, Rowczenio DM, Whelan CJ, Ashworth MA, Gillmore JD, Hawkins PN and Moon JC. Occult transthyretin cardiac amyloid in severe calcific aortic stenosis: prevalence and prognosis in patients undergoing surgical aortic valve replacement. Circ Cardiovasc Imaging 2016; 9: e005066.
[29] Ternacle J, Krapf L, Mohty D, Magne J, Nguyen A, Galat A, Gallet R, Teiger E, Cote N, Clavel MA, Tournoux F, Pibarot P and Damy T. Aortic stenosis and cardiac amyloidosis: JACC review topic of the week. J Am Coll Cardiol 2019; 74: 2638-2651.
[30] Senapati A, Sperry BW, Grodin JL, Kusunose K, Thavendiranathan P, Jaber W, Collier P, Hanna M, Popovic ZB and Phelan D. Prognostic implication of relative regional strain ratio in cardiac amyloidosis. Heart 2016; 102: 748-754.
[31] Ternacle J, Bodez D, Guellich A, Audureau E, Rappeneau S, Lim P, Radu C, Guendouz S, Couetil JP, Benhaiem N, Hittinger L, Dubois-Rande JL, Plante-Bordeneuve V, Mohty D, Deux JF and Damy T. Causes and consequences of longitudinal LV dysfunction assessed by 2D strain echocardiography in cardiac amyloidosis. JACC Cardiovasc Imaging 2016; 9: 126-138.
[32] Hu K, Liu D, Nordbeck P, Cikes M, Stork S, Kramer B, Gaudron PD, Schneider A, Knop S, Ertl G, Bijnens B, Weidemann F and Herrmann S. Impact of monitoring longitudinal systolic strain changes during serial echocardiography on outcome in patients with AL amyloidosis. Int J Cardiovasc Imaging 2015; 31: 1401-1412.
[33] Koyama J and Falk RH. Prognostic significance of strain Doppler imaging in light-chain amyloidosis. JACC Cardiovasc Imaging 2010; 3: 333-342.
[34] Lo Q, Haluska B, Chia EM, Lin MW, Richards D, Marwick T and Thomas L. Alterations in regional myocardial deformation assessed by strain imaging in cardiac amyloidosis. Echocardiography 2016; 33: 1844-1853.
[35] Buss SJ, Emami M, Mereles D, Korosoglou G, Kristen AV, Voss A, Schellberg D, Zugck C, Galuschky C, Giannitsis E, Hegenbart U, Ho AD, Katus HA, Schonland SO and Hardt SE. Longitudinal left ventricular function for prediction of survival in systemic light-chain amyloidosis: incremental value compared with clinical and biochemical markers. J Am Coll Cardiol 2012; 60: 1067-1076.
[36] Quarta CC, Solomon SD, Uraizee I, Kruger J, Longhi S, Ferlito M, Gagliardi C, Milandri A, Rapezzi C and Falk RH. Left ventricular structure and function in transthyretin-related versus light-chain cardiac amyloidosis. Circulation 2014; 129: 1840-1849.
[37] Barros-Gomes S, Williams B, Nhola LF, Grogan M, Maalouf JF, Dispenzieri A, Pellikka PA and Villarraga HR. Prognosis of light chain amyloidosis with preserved LVEF: added value of 2D speckle-tracking echocardiography to the current prognostic staging system. JACC Cardiovasc Imaging 2017; 10: 398-407.